Pergamon

Scripta Materialia, Vol. 34, No. 8, pp. 1331–1336, 1996
Elsevier Science Ltd

1359-6462/96 $12.00 + .00

SSDI 0956-716X(95)00656-7

T-P PHASE DIAGRAM OF THE Mn-H SYSTEM AT PRESSURES TO 4.4 GPa AND TEMPERATURES TO 1000°C

V.E. Antonov[1], T.E. Antonova[1], N.A. Chirin[1], E.G. Ponyatovsky[1], M. Baier[2] and F.E. Wagner[2]

[1]Institute of Solid State Physics, Russian Academy of Sciences, 142432 Chernogolovka, Moscow District, Russia

[2]Physics Department, Technical University of Munich, D-85747 Garching, Germany

(Received September 7, 1995)

Introduction

At atmospheric pressure, there are 4 allotropic modifications of manganese: α-Mn with a complex cubic lattice at temperatures up to about 710°C, β-Mn with another complex cubic lattice at temperatures between 710°C and 1090°C, *fcc* γ-Mn betweeen 1090°C and 1137°C and *bcc* δ-Mn between 1137°C and the melting point at 1244°C. Both the melting temperature and the temperatures of the transitions between the different modifications increase with pressure (1).

Under high pressures of hydrogen and at temperatures up to about 350°C, manganese was found to form ε-hydrides with an *hcp* metal lattice (2–4). Later, Fukai et al. (5) synthesized *fcc* (γ) hydrides of manganese at pressures above 1.2 GPa and temperatures between 900 and 1200°C by an exchange reaction with $LiAlH_4$. Since γ-Mn is the stable phase in this temperature range, these hydrides were considered as solid solutions of hydrogen in γ-Mn. Rather surprisingly, Filipek et al. (6) then found that, in an atmosphere of about 1 GPa of molecular hydrogen, manganese forms γ-hydrides already at temperatures as low as 325°C. In further experiments with high pressure cells presumably similar to those used in (5), the lower boundary of stability of the γ-hydrides in the $T-P$ plane was found to shift towards lower temperatures with increasing pressure, namely down to about 470°C at 3 GPa (7), which does, however, not include the γ-region observed by Filipek et al. (6). The chemical potential of the hydrogen in the experiments described in (5,7) may, however, have differed from that of molecular hydrogen at the same temperature and pressure. Therefore the phase boundaries and even the topology of the $T-P$ diagram determined in these experiments may be different from those pertaining to an atmosphere of molecular hydrogen.

In the present work, the phase transformations in the Mn–H system were studied in an atmosphere of gaseous hydrogen within the temperature and pressure interval comprising the stability regions of the α, β, γ and ε phases.

Experimental

The phase diagram of the Mn–H system was constructed from the results of a room temperature X-ray examination of powder samples using a DRON 2.0 diffractometer, FeK_α radiation, and photographic

TABLE 1
Hydrogen Content (H/Mn atomic ratio), Conditions of Synthesis (Hydrogen Pressure P_{H_2}, Temperature T and Exposure Time τ), Unit Cell Parameters of the Metal Sublattice at Room Temperature (a and c) and Volume per Mn Atom (V_a) for α-Mn and Some Mn-H High Pressure Phases

Metal lattice	H/Mn	P_{H_2} (GPa)	T (°CC)	τ	a (nm)	c (nm)	$V_a \times 10^3$ (nm^3)
α-Mn	0	Initial sample			0.8912	—	12.20
α-Mn	0.06	0.6	650	20 min	0.8949	—	12.36
β-Mn	0.08	0.6	800	10 min	0.6342	—	12.75
γ (*fcc*)	0.36	0.8	1000	10 min	0.3801	—	13.73
ε (*hcp*)	0.86	2.6	350	24 h	0.2694	0.4357	13.69

registration. The samples were exposed to molecular hydrogen at a given pressure and temperature and rapidly cooled to ambient temperature before removal from the high pressure cell. Cooling to a temperature of 60°C took less than 15 s; at this temperature and ambient pressure no change in the phase composition of the Mn–H samples was observed during hours.

The starting material placed into the high pressure cell was always an ε-hydride of manganese with the atomic ratio H/Mn $\approx$ 0.85. This hydride had been prepared previously by exposing powdered manganese metal of 99.99 wt% purity and a grain size of less than 100 μm to $P_{H_2} = 2.6$ GPa at $T = 350$°C for 24 h. The hydrogen content of this hydride and of some of the Mn–H samples obtained in the course of this work was determined with an accuracy of 1 % by hot extraction at temperatures up to 500°C (Table 1).

To compress gaseous hydrogen at temperatures up to 350°C, we used the method described in (8), with heptane as the liquid gate and AlH_3 as the solid hydrogen donor. The aluminium trihydride powder had a purity of 99.8 wt% and a grain size of 30–40 μm. It was prepared by desolvation of $AlCl_3$ etherate in the presence of small amounts of $LiAlH_4$ (9). For pressures up to 2 GPa, a hydrostatic chamber of the piston-cylinder type was used to apply the pressure to the sample cell, and the pressure and temperature were measured with an accuracy of $\pm$0.05 GPa and $\pm$5°C, respectively. Higher pressures were produced in quasihydrostatic chambers of the toroid type, for which the accuracy of the pressure and temperature determination was $\pm$0.2 GPa and $\pm$10°C, respectively. The experiments above 350°C were carried out in toroid-type high pressure chambers at all pressures. In these cases the temperature and pressure were measured with an accuracy of $\pm$20°C and $\pm$0.2 GPa, respectively.

With the high pressure cells described in (8) one cannot reach temperatures above 500–600°C due to thermal decomposition of the organic or silicon-organic liquid used to prevent hydrogen leaks and to separate the hydrogen from the donor material. To attain higher temperatures, the cell was therefore modified as shown in Fig. 1. The teflon capsule used previously (8) is replaced by a copper capsule closed by a copper plug. To obtain a tight seal, the gap between the capsule and the plug is filled with gallium, which is liquid at ambient temperature and diffuses into the copper when the temperature is raised, forming Cu–Ga alloys of increasing thermal stability as its concentration in the copper matrix decreases (10). Both Cu and Ga are largely impermeable to hydrogen. The hydrogen released on thermal decomposition of the AlH_3 is thus sealed into the capsule at all temperatures below the melting point of copper at the respective pressure. The dead space in the capsule is filled with kaolin wool. A mica washer prevents the mixing of the kaolin wool with the AlH_3. Kaolin wool does not react with H_2, Mn or Cu in the temperature and pressure range of interest. Due to the hardness of its fibres, it remains porous even at high pressures, leaving enough room for the hydrogen gas inside the capsule and ensuring good access of the hydrogen to the sample.

The described cells are placed into a quasihydrostatic high pressure chamber and compressed to between 0.4 and 1.5 GPa before being heated to about 250°C, where the AlH_3 decomposes (Fig. 2) and liberates the hydrogen. After that, one can change the pressure and temperature to any desired value below the

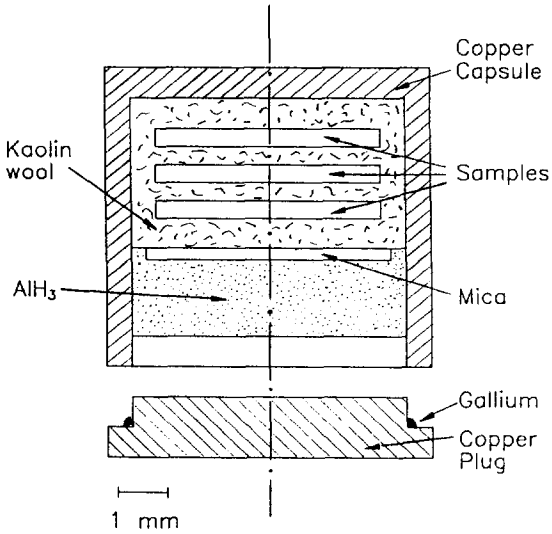

Figure 1. Schematic diagram of the high pressure cell using aluminium trihydride as a solid hydrogen source.

melting point of copper, except for two regions in the $T-P$ diagram, which are shaded in Fig. 2. In the wedge-shaped region at high pressures and at temperatures ranging from about 300°C up to about 50°C below the decomposition curve of aluminium hydride, AlH_3 might form again from Al and H_2 gas (11). The second region in which the cell could not be operated extends to the left from the isobar at about 0.7 GPa and above the melting curve of Al (Fig. 2). For an unknown reason, the aluminium powder used to merge under these conditions, and the melt spread out over the kaolin wool and the sample. Usually, a thin layer of aluminium oxide appears to form on the surface of the aluminium particles resulting from the decomposition of the AlH_3, thus impeding the merging. As can be seen from the points in Fig. 2, the molten aluminium powder did not merge at pressures exceeding 0.8 GPa, nor did it at ambient pressure.

One cannot rule out that the observed merging at pressures below 0.7 GPa is connected with the formation of yet unknown Al–H phases at high temperatures. In experiments with high pressure cells filled

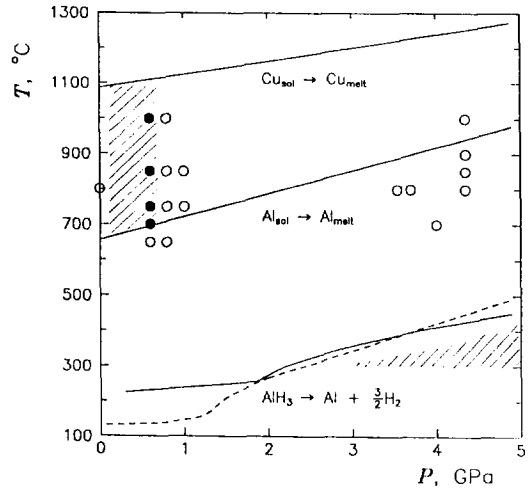

Figure 2. Phase transformations in the constituents of the copper high pressure cell. The fully drawn decomposition curve of AlH_3 is from (15), the dashed one from (11). The melting curves of Al and Cu are from (1). Shaded areas depict the regions where the cells could not be used with AlH_3 as the hydrogen donor. The points show the behaviour of the metallic Al formed upon decomposition of AlH_3 within the cell: open symbols indicate that the Al remained an inert powder, filled ones that the molten Al merged and formed an ingot.

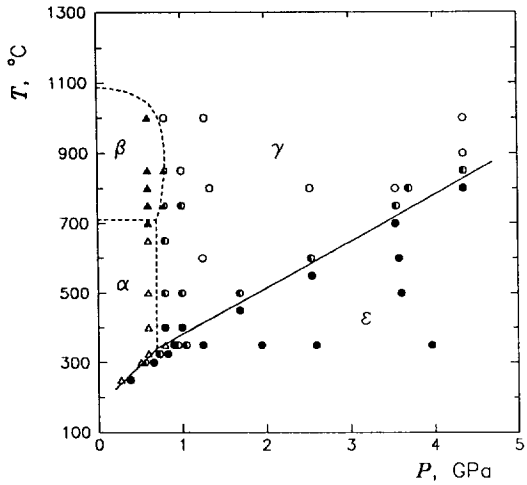

Figure 3. $T-P$ phase diagram of the Mn–H system. Open triangles represent solid solutions of hydrogen in α-Mn, filled triangles solid solutions in β-Mn, open circles hydrides on the base of γ-Mn, and filled circles ε-hydrides with *hcp* metal lattice. Half filled symbols represent samples consisting of a mixture of the corresponding phases.

completely with AlH_3, the Al formed in the decomposition of AlH_3 was therefore heated for 10 min to a temperature of 1000°C at 0.6 and 0.8 GPa, respectively, and then quenched to −180°C. As expected, at 0.6 GPa the Al had merged and at 0.8 GPa it had not. An X-ray analysis of the resulting specimens at ambient pressure and −170°C, however, revealed nothing but aluminium with an unchanged lattice parameter in both cases.

In the experiments at $P_{H_2} < 0.8$ GPa and $T > 700$°C, no AlH_3 was used at all. The cells were completely filled with ε-phase manganese hydride, which on heating released enough hydrogen to provide an excess of H_2 gas in addition to the β and γ phases stable at these temperatures and pressures.

Results and Discussion

The results of the phase identification of the quenched Mn–H samples are given in Fig. 3 and Table 1. Only primary solid solutions of hydrogen, with a maximum hydrogen concentration of the order of a few atomic percent, were formed on the base of the α and β modifications of manganese. These solid solutions are stable only below about 0.8 GPa. At higher pressures, the stability fields of the ε and γ hydrides in the phase diagram make contact and the temperature of the $\varepsilon \Leftrightarrow \gamma$ equilibrium increases monotonically with pressure. The ε and γ hydrides are nonstoichiometric phases. In the studied $T-P$ interval (Fig. 3), their hydrogen content increases with pressure from H/Mn $\approx$ 0.35 to $\approx$ 0.5 for the γ hydride, and from H/Mn $\approx$ 0.8 to $\approx$ 0.95 for the ε hydride.

The data points in Fig. 3 were obtained as follows: The starting material was always ε-$MnH_{\approx 0.85}$, and each experiment began with the decomposition of AlH_3 at a temperature of about 250°C and a pressure below 1.5 GPa, within the stability region of the ε-hydride of manganese. For the points at temperatures up to 350°C, the pressure was then increased above the desired setting and kept there for about an hour. Thereafter it was lowered again to the final value, at which it was left for 6 h to attain equilibrium at the given pressure and temperature. To obtain the data points at higher temperatures, the temperature was increased at a constant or somewhat increasing pressure, and the time of exposure to the final temperature and pressure varied from 2 h at 400°C to 10 min at 1000°C. These procedures were followed to avoid ambiguities in the final state of the samples due to hysteresis effects. The ε-hydride was chosen as the starting material because it has the highest hydrogen content among the Mn–H phases. One therefore expects that the lines of its decomposition to the α and γ phases are closer to the lines of the phase equilibria than the lines of

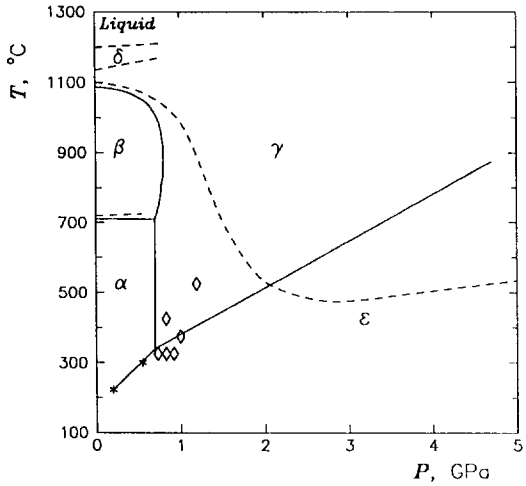

Figure 4. $T-P$ phase diagram of the Mn–H system compared with literature data. Solid lines are phase boundaries determined in the present work, dashed lines phase boundaries according to (7). Diamonds depict the conditions of synthesis of γ-hydrides reported in (6), asterisks the pressures of the $\varepsilon \rightarrow \alpha$ transition according to (15).

its formation (an analysis of the hysteresis phenomena in metal-hydrogen systems is given, for example, in (12–13)).

Since the phase rule allows only single-phase fields in the $T-P$ diagram of the Mn–H system, the points in Fig. 3 that represent two-phase states must refer to non-equilibrium mixtures, in which the respective phase transformation occurred only partly, but should have been completed if equilibrium had been reached. The phase boundary lines in Fig. 3 were plotted to contour only single phase points in the ε, α and β fields, respectively. In the $T-P$ phase diagram obtained in this way, there are two points of ternary phase equilibrium, namely $(\alpha + \varepsilon + \gamma)$ at approximately 0.7 GPa and 350°C and $(\alpha + \beta + \gamma)$ at approximately 0.7 GPa and 700°C.

In Fig. 4 the phase diagram constructed as described above is compared with the available literature data. It is worth noting that the low-temperature boundary of the γ-region given by Fukai (7) is in fair agreement with the boundary now obtained in an atmosphere of molecular hydrogen. This suggests that the high temperature phase equilibria reached by hydrogen exchange with $LiAlH_4$ are, indeed, similar to those in an atmosphere of H_2 gas.

The line of the $\varepsilon \rightarrow \alpha$ transition obtained in the present work agrees well with the midpoints of the plateaus of the isotherms of hydrogen solubility in manganese (asterisks in Fig. 4) measured at 227 and 304°C with high accuracy at decreasing hydrogen pressure (14).

The $T-P$ range in which Filipek et al. (6) obtained the γ manganese hydride (diamonds in Fig. 4) is consistent with the present phase diagram, but we could not obtain the γ phase by exposing α-Mn to increasing hydrogen pressures between 0.8 and 1.2 GPa at 350°C for periods between a few hours and 3 days. Instead of the formation of the γ phase, the direct transformation of the α phase into the ε-phase was observed. In our samples, partial formation of the γ phase at 350°C occurred only on decreasing pressure (Fig. 3). We suggest that this discrepancy with the results of Filipek et al. (6) is due to the fact that the $\varepsilon \Leftrightarrow \gamma$ transformation is very sluggish at pressures between 0.5 and 1.5 GPa. Hence the final state of the samples may depend strongly on the presence of defects and local stresses.

Summary

The Mn–H phase diagram was constructed from the results of a room temperature X-ray study of powder samples exposed to molecular hydrogen at a given pressure and temperature. Within the studied $T-P$

interval, manganese and hydrogen were shown to form four different phases: the primary solid solutions on the basis of the α and β allotropic modifications containing only a few atomic percent of hydrogen, a hydride on the basis of the γ (*fcc*) modification and a hydride with an *hcp* (ε) metal lattice. The phase diagram is characterized by two triple points, $(\alpha + \varepsilon + \gamma)$ at approximately 0.7 GPa and 350°C and $(\alpha + \beta + \gamma)$ at approximately 0.7 GPa and 700°C. The temperature of the $\varepsilon \rightarrow \gamma$ transition increases linearly with pressure and reaches $\approx$ 850°C at 4.4 GPa.

Acknowledgments

This work has been supported in part by the NATO Linkage Grant No. 921403 and by the Grant No. REP300 from the International Science Foundation and the Russian Government.

References

1. E. Yu. Tonkov, High Pressure Phase Transitions, Gordon and Breach, Philadelphia (1992).
2. M. Krukowski and B. Baranowski, Roczniki Chem. 49, 1183 (1975).
3. E. G. Ponyatovsky and I. T. Belash, Dokl. Akad. Nauk SSSR 224, 607 (1975) [in Russian].
4. I. T. Belash, B. K. Ponomarev, V. G. Thiessen, N. S. Afonikova, V. Sh. Shekhtman and E. G. Ponyatovsky, Fiz. Tverd. Tela 20, 422 (1978) [in Russian].
5. Y. Fukai, H. Ishikawa, T. Goto, J. Susaki, T. Yagi, J. L. Soubeyrox and D. Fruchart, Z. Phys. Chem. N. F. 163, 479 (1989).
6. S. M Filipek, S. Majchrzak, A. B. Sawaoka and M. Cernansky, High Pressure Research 7, 271 (1991).
7. Y. Fukai, The Metal-Hydrogen System, Springer, Berlin (1993).
8. E. G. Ponyatovsky, V. E. Antonov and I. T. Belash, Problems in Solid-State Physics, p. 109, eds. A. M. Prokhorov and A. S. Prokhorov, Mir, Moscow (1984).
9. F. M. Brower, N. E. Matzek, P. F. Reigler, H. W. Rinn, C. B. Roberts, D. L. Schmidt, J. A. Snover and K. Terada, J. Amer. Chem. Soc. 98, 2450 (1976).
10. M. Hansen and K. Anderko, Constitution of Binary Alloys, McGraw-Hill, New York (1958).
11. S. K. Konovalov and B. M. Bulychev, Zh. Neorgan. Khim. 37, 2641 (1992) [in Russian].
12. E. Wicke and H. Brodowsky, Topics in Applied Physics vol. 29, Hydrogen in Metals II, p. 73, eds. G. Alefeld and J. Völkl, Springer, Berlin (1978).
13. B. Baranowski and K. Bocheńska, Z. Phys. Chem. N. F. 45, 140 (1965).
14. B. Baranowski, Z. Phys. Chem. N. F. 114, 59 (1979).
15. I. T. Belash, Doctoral Thesis, Institute of Solid State Physics, Chernogolovka (1976) [in Russian].